HYDROLOGICAL PROCESSES
Hydrol. Process. **15**, 2085–2099 (2001)
DOI: 10.1002/hyp.280

Spatial resolution sensitivity of catchment geomorphologic properties and the effect on hydrological simulation

Dawen Yang,[1]* Srikantha Herath[2] and Katumi Musiake[2]

[1] *Department of Civil Engineering, University of Tokyo, 7-3-1 Hongo, Bunkgo-Ku, Tokyo 113-8656, Japan*
[2] *Institute of Industrial Science, University of Tokyo, Meguro-Ku, Tokyo 153-8505, Japan*

Abstract:

The geomorphologic area function and width function that characterize the forms of hillslope and river networks are two key parameters employed in the GBHM (geomorphology-based hydrological model) for representing the hydrological processes together with other spatial information. One fundamental issue on the use of the geomorphologic properties is the spatial resolution sensitivity in both the threshold area for river network generation and digital elevation model (DEM) resolution. The threshold area is the minimum drainage area required to initiate the river; the DEM resolution depends on the available elevation data. In the present study, multifractal analysis was used to investigate the sensitivity of width functions extracted by different threshold areas and the sensitivity of area functions extracted from various resolutions of DEMs. Fifteen Japanese catchments were selected for the sensitivity analysis based on 250 m mesh DEM data. It was found that the river networks generated with larger threshold areas tend to lose the detailed scaling information. When the DEM mesh size increases, the river networks extracted with the same threshold area become sparser and the topography tends to be flat and scaling structures of the area functions become simpler. The runoff generations of the GBHM were influenced by the DEM resolution. The effect of the DEM resolution on the hydrological response is related to the temporal resolution with more influence on the hourly response compared with the daily response. From the relation between the scaling structure expressed by the multifractal spectrum and the hydrological response of a catchment, it was found that the detailed scaling information had more effect on the hydrological response of higher temporal resolution. Copyright © 2001 John Wiley & Sons, Ltd.

KEY WORDS sensitivity analysis; multifractal; area function; width function; hydrological simulation

INTRODUCTION

Physically-based models employ topographical and geomorphologic parameters that characterize the landforms for representation of the hydrological processes. The topographical index $\ln(a/\tan\beta)$ (where a is drainage area per unit contour length and β is slope) is used in the TOPMODEL (Beven, 1989), which is a key parameter for determining the runoff generation. Geomorphology research has identified a number of geometric regularities, such as Horton's laws, width function and area function, in hillslope and river network forms, which can be employed for describing catchment hydrological response (Mesa and Mifflin, 1986; Robinson *et al*., 1995; Yang *et al*., 1997; Yen and Lee, 1997; Herath *et al*., 1999). The GBHM represents a catchment using hillslopes extracted by using the flow interval–hillslope scheme (Yang *et al*., 1998, 2000). The topography is represented by slope length derived from the area function and width function, slope angle and elevation.

The landform parameterizations rely on the integrity of the digital elevation models (DEMs) in both model principle and data resolution (Moore *et al*., 1991). O'Callaghan and Mark (1984) defined a DEM as any numeric or digital representation of the elevation of the land surface. There are mainly three types of DEM: (1) grid (regular square grid) based DEM (O'Callaghan and Mark, 1984; Tarboton *et al*., 1991),

* Correspondence to: D. Yang, Department of Civil Engineering, University of Tokyo, 7-3-1 Hongo, Bunkgo-Ku, Tokyo 113-8656, Japan.
E-mail: dyang@hydra.t.u-tokyo.ac.jp

Received 10 February 2000
Accepted 2 June 2000

which is the most common approach; (2) TIN (triangular irregular networks) based DEM (Palacios-Velez and Cuevas-Renaud, 1986); and (3) contour based DEM (Moore *et al*., 1988). The most common method of extracting river networks from DEMs is the flow accumulation procedure that specifies a threshold area to initiate a river. Two general methods have been used to simulate network sources in DEMs: a constant threshold area (O'Callaghan and Mark, 1984; Tarboton *et al*., 1991) and a slope-dependent threshold area (Dietrich *et al*., 1993). Although Montgomery and Foufoula-Georgiou (1993) compared the two methods and concluded that a slope-dependent threshold area is more appropriate for defining the extent of river networks, no proportional constant had been found for the area–slope threshold controlling river initiation. In the present study, the flow accumulation method that was provided by ARC/INFO software is used to extract the river networks from the grid based DEM. The flow direction is defined as the steepest one of eight possible paths for each square grid and a constant threshold is used to initiate the river. The threshold is the minimum accumulative area that is required to start the 'river'. The generated 'river' from a DEM may not agree with the actual river. This study focuses on examining the sensitivity of geomorphologic parameters to the threshold value rather than detecting the actual river.

From the catchment hydrological response point of view, the catchment scaling property is the characteristics of runoff accumulation, which can be estimated from Horton's ratios, area functions and width functions. Assuming a uniform effective rainfall and a constant flow velocity over the catchment, the pattern of flow accumulation is given by the area function. The area function shows the one-dimensional scaling structure with respect to flow distance from the catchment outlet. The scaling structure of a catchment is recognized to be a fractal or multifractal (Barbera and Rosso, 1989; Rinaldo *et al*., 1993; Nikora and Sapozhnikov, 1993; Maritan *et al*., 1996). The general scaling property is usually expressed by the power law whose exponent is the fractal dimension. Rinaldo *et al*. (1993) suggested that width function is made up of subsets with different fractal dimensions. Width functions are multifractal and a single fractal dimension is inadequate to describe their scaling structures. multifractals are characterized by a spectrum of fractal dimensions called singularity spectrums (Feder, 1998). It illustrates the full picture of the scaling properties of what is described. Multifractal analysis has been used to study the scaling property of the width function (Rinaldo *et al*., 1993; Marani *et al*., 1994). Veneziano *et al*. (1995) discussed the numerical problems of the multifractal analysis method, especially on the singularity spectrum of width functions of river basins.

The digital elevation data are available at a variety of resolutions derived from various original data sources. Walker and Willgoose (1999) suggested that the accuracy of published DEM data is very questionable for estimating the topographical and geomorphologic parameters. It is necessary to analyse the sensitivity of topographical and geomorphologic parameters to the DEM resolutions when they are used in hydrological simulations. Zhang and Montgomery (1994) investigated the effect of DEM resolution on the topographical index and the simulated hydrological response of the TOPMODEL to a simple short-duration rainfall event in two catchments studied, which have areas of 0·3 km^2 and 1·2 km^2 respectively. Their results showed that the topographical index is very sensitive to the grid size. In general, increasing the coarseness of DEM resolution tended to decrease the mean depth from surface to the water table and increase the peak flow (Zhang and Montgomery, 1994). Wolock and Price (1994) also examined the sensitivity of the topographical index and the hydrological response of the TOPMODEL to the DEM resolution in 71 quadrangular study areas that have sizes of 10 by 14 km each. Single values of the model parameters and a single 5-year time series of daily rainfall were the model inputs. It was concluded that increasing the DEM grid size on average tended to decrease the mean depth to the water table and increased the ratio of overland flow to total flow, the variance of daily flow the skew of daily flow and the maximum daily flow (Wolock and Price, 1994).

In the present study, the sensitivity of width function to the threshold area and the sensitivity of the area function to the DEM resolution were investigated using the multifractal analysis in 15 Japanese catchments. The digital elevation data used in the study are originally in 250 m resolution; 500 m and 1000 m DEMs were generated from the original one. The effect of DEM resolution on catchment hydrological responses simulated by the GBHM is discussed in this paper.

STUDY AREAS AND GEOMORPHOLOGIC PARAMETERS

The digital elevation data used in this study were produced by the Japan Geographical Survey Institute. The study areas include 15 catchments located in Kyushu, Shikoku, Hokuriku and Kanto regions of Japan (Figure 1). The catchment areas range from 464 km^2 to 3049 km^2. Most of them are complete basins that drain to the sea, only three in Kanto region are the subcatchments of the Tone River basin.

The most common geomorphologic parameters include drainage density and Horton's ratios. The drainage density is the ratio of total length of streams to the area of the catchment. The total length of streams can be calculated by the sum of lengths of all stream cells according to the flow directions in a grid based DEM. Using Strahler's stream order system (1952), Horton's ratios, i.e. bifurcation ratio R_B, length ratio R_L, and area ratio R_A, are defined by

$$R_B = \frac{N_\omega}{N_{\omega+1}} \tag{1a}$$

$$R_L = \frac{L_{\omega+1}}{L_\omega} \tag{1b}$$

$$R_A = \frac{A_{\omega+1}}{A_\omega} \tag{1c}$$

where N_ω, L_ω and A_ω respectively denote the number, average length and average catchment area of streams of order ω. Based on Horton's ratios, the fractal dimension D is defined as (Ichoku *et al*., 1996)

$$D = \frac{\log R_B}{\log R_L} \tag{2}$$

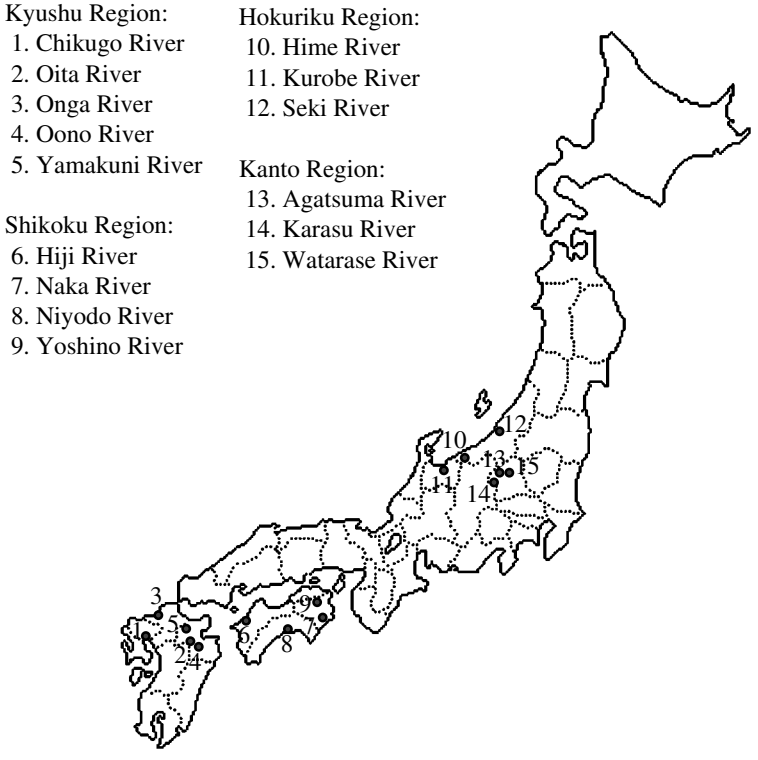

Figure 1. Locations of study areas

For all study catchments, the river networks were generated using different threshold areas from the DEM. Based on the generated river networks, river density and Horton's ratios were calculated. The fractal dimensions were calculated by Equation (2). Figure 2 shows that the river density varies linearly with threshold areas in a log–log plot, which suggests a common power law relationship between the drainage density and threshold area. Horton's ratios and the fractal dimension derived from Horton's ratio vary irregularly with the threshold areas. The fractal dimensions of some study catchments are greater than 2, such as the Seki River in Figure 3. The explanation of the greater than 2 fractal dimension estimates is that the constant threshold is improper for extraction of river networks in mountainous catchments because initiation of a river in the mountainous area depends on both slope and accumulative area (Helmlinger *et al*., 1993; Ichoku *et al*., 1996).

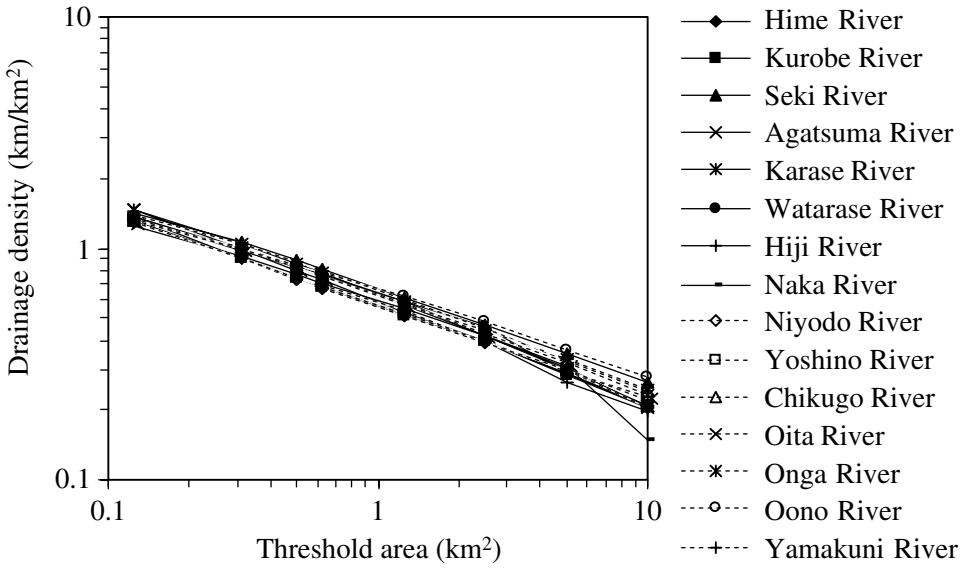

Figure 2. Effect of threshold area on the drainage density

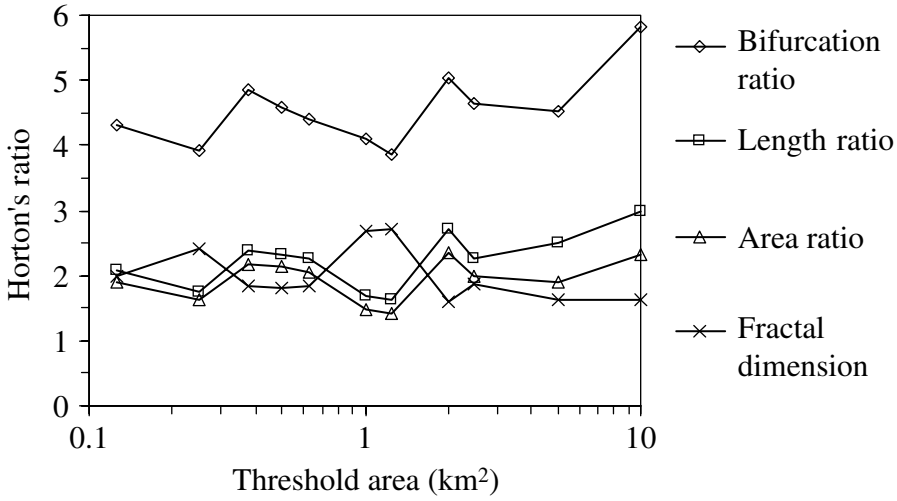

Figure 3. Effect of threshold area on Horton's ratios and fractal dimension (the Seki River)

As shown in Figure 4, the width function W(x) is defined as the frequency distribution of streams with respect to flow distance from the outlet. Mathematically, the width function is given by

$$W(x) = \sum_{i=1}^{N} n_i(x, d_{i_{min}}, d_{i_{max}}) \tag{3a}$$

where x is the flow distance along the river from the catchment outlet; i is the number of a stream link; N is the total number of stream links; $d_{i_{min}}$ and $d_{i_{max}}$ are the distances of the downstream end and the upstream end of stream link i from the outlet, respectively; the function n_i is defined by

$$n_i(x, d_{i_{min}}, d_{i_{max}}) = \begin{cases} 1, & d_{i_{min}} < x \leq d_{i_{max}} \\ 0, & \text{otherwise} \end{cases} \tag{3b}$$

The width functions vary with the threshold areas specified for the river network generations. The area function A(x) is the distribution of the accumulative area with respect to flow distance from the outlet, defined as

$$A(x) = \frac{A_c(x) - A_c(x + \Delta x)}{\Delta x} \tag{4}$$

where $A_c(x)$ and $A_c(x + \Delta x)$ are the cumulative areas which drain into downstream at distance x and $x + \Delta x$, respectively. The area function can be uniquely extracted from the DEM. The width and area functions were normalized in the multifractal analysis. The maximum flow distance is normalized to 1, and the integral of the curve (i.e. the area covered by the curve) is normalized to 1. The variations of width functions with the threshold areas were examined using 250 m resolution DEMs. Figure 5 shows an example of the changes of the normalized width function extracted from different threshold areas in the Seki River. The area functions vary with the DEM resolutions, and its sensitivity was examined by different DEMs with resolutions of 250 m, 500 m, and 1000 m. Figure 6 shows an example of the area functions extracted from the DEMs with different resolutions. The variations of both width function and area function can be seen from Figures 5 and 6, but a tool is necessary to evaluate these changes.

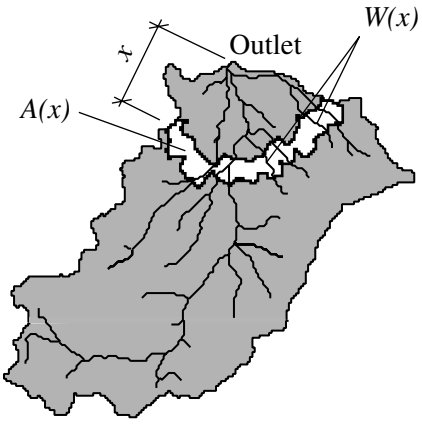

Figure 4. The definition of width function and area function

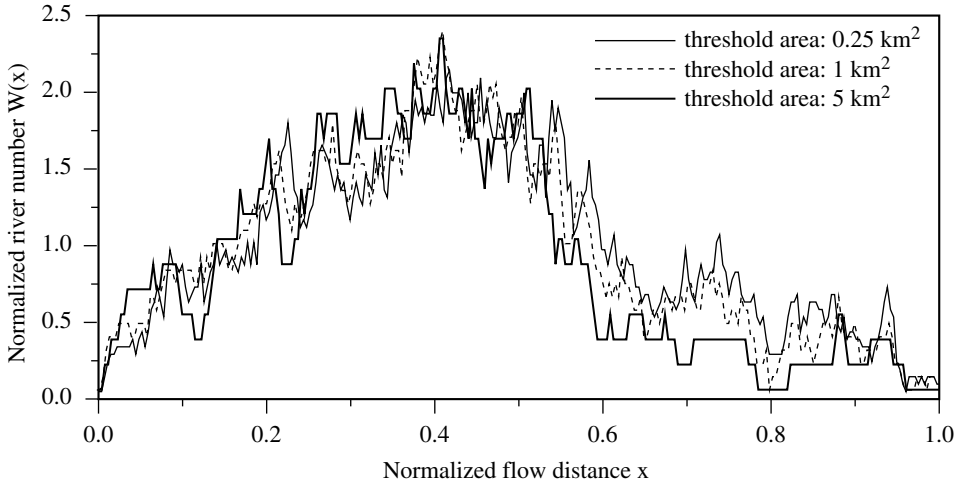

Figure 5. Normalized width functions of the Seki River extracted from different threshold areas

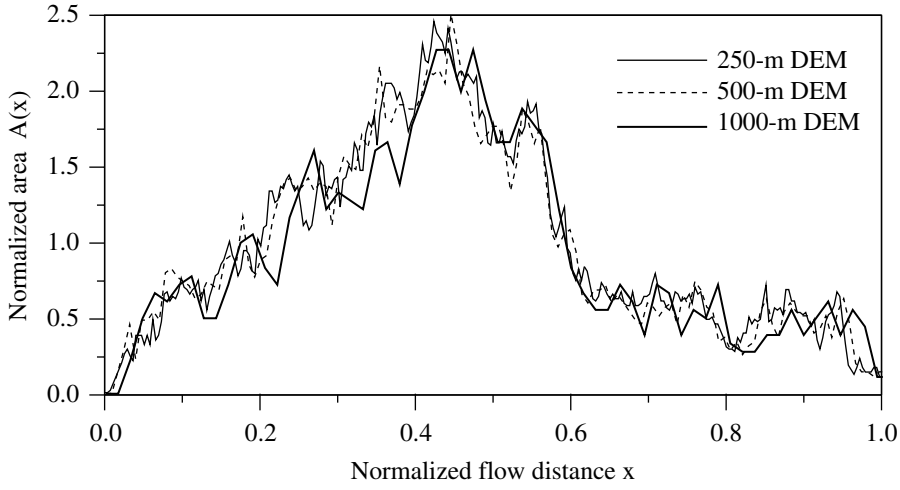

Figure 6. Normalized area functions of the Seki River extracted from different resolutions of DEMs

SENSITIVITY ANALYSIS OF WIDTH FUNCTION AND AREA FUNCTION USING MULTIFRACTALS

Methodology

For the normalized width function or area function, let $P_\varepsilon(x)$ be the integral over the box of size ε centred at x. The property P of interest is the scaling exponent $\alpha(x)$ defined as

$$\alpha(x) = \lim_{\varepsilon \to 0} \frac{\log P_\varepsilon(x)}{\log \varepsilon} \tag{5}$$

The spectrum $\{\alpha, f(\alpha)\}$, with $f(\alpha)$ the Hausdorff dimension of the set composed of points x with $\alpha(x) = \alpha$, is the multifractal spectrum, or singularity spectrum. Larger $f(\alpha)$ means many points have the same singularity strength. Various procedures have been developed to estimate $\{\alpha, f(\alpha)\}$. In Chhabra and Jensen's procedure

(1989), a normalized measure is defined by the qth moments of P, given by

$$\mu_i(q, \varepsilon) = \frac{[P_i(\varepsilon)]^q}{\sum_j [P_j(\varepsilon)]^q} \tag{6}$$

The entropy S of the measures is given as

$$S(\varepsilon) = -\sum_i \mu_i(q, \varepsilon) \log \mu_i(q, \varepsilon) \tag{7}$$

From the definition of information dimension related to entropy, the Hausdorff dimension of the measures is given by

$$f(q) = \lim_{\varepsilon \to 0} \frac{\sum_i \mu_i(q, \varepsilon) \log \mu_i(q, \varepsilon)}{\log \varepsilon} \tag{8}$$

Reviewing Equation (5), the singularity strength α, with respect to the measure $\mu(q, \varepsilon)$, is given by

$$\alpha(q) = \lim_{\varepsilon \to 0} \frac{\sum_i \mu_i(q, \varepsilon) \log P_i(\varepsilon)}{\log \varepsilon} \tag{9}$$

The procedure of estimating α and $f(\alpha)$ is to calculate the slopes of $\sum_i \mu_i(q, \varepsilon) \log P_i(\varepsilon)$ against $\log \varepsilon$ and $\sum_i \mu_i(q, \varepsilon) \log \mu_i(q, \varepsilon)$ against $\log \varepsilon$ by the linear regressions, respectively.

In applications of the multifractal analysis, two sources of error lie in largely unknown biases introduced by the finiteness of data available, and the finite range of length scales inherent in gathered data. In order to investigate this problem, the analytical multifractal spectrum of the parabola function $g(x) = 2x - x^2$ was compared with the numerical estimates using Chhabra and Jensen's approach. In the numerical computation, the normalized function was used, i.e. the function was normalized on the interval [0, 1] and the integral over the interval is 1. The linear regression correlation coefficients were set to be larger than 0·9 for keeping high confidence. The range of q considered in each analysis is from -10 to 10 in an interval of 0·2.

Considering the interval [0, 2], the integral of this parabola on any interior point over $[x - \varepsilon/2, x + \varepsilon/2]$ is $P_\varepsilon(x) = (2x - x^2)\varepsilon - \varepsilon^3/12$, the singularity strength is $\alpha = 1$. The Hausdorff dimension of this singular is 1 because the distribution of this singular is uniform. In both ends, $P_\varepsilon(0) = \int_0^\varepsilon g(x)dx = P_\varepsilon(2) = \int_{2-\varepsilon}^2 g(x)dx = \varepsilon^2(1 - \varepsilon/3)$, the singularity strength $\alpha = 2$. Because there are only two points, the Hausdorff dimension is 0. Therefore, the multifractal spectrum of this parabola contains two points (1,1) and (2,0) which characterize the interior distributions and the two ends respectively. In the numerical solution, the following two steps were made: (1) using enough data samples (2001 discrete data points were used) to find the appropriate scale range; (2) then taking this scale range to find the minimum number of data points needed for the numerical solution. In the first step, when the scale range is increased to [1/2000, 2/2000,. . ., 35/2000] the spectrum becomes very close to the point (1,1) (see Figure 7); taking this scale range, it was found that the spectrum became very close to point (1,1) when the data number is more than 550 in the second step (see Figure 8). The numerical procedure focuses on the interior part with interest.

From this example, it was found that the unreal points in the spectrum were obtained by the numerical estimations with insufficient data samples or narrow scale ranges. The error introduced by the scale range is relatively smaller. By increasing the data samples and expanding the scale range, the real multifractal spectrum can be correctly calculated by Chhabra–Jensen's algorithms.

In the case of catchment width functions and area functions, the number of data samples is limited by the DEM resolutions. For example, the width function or area function of the Seki River extracted from 250 m

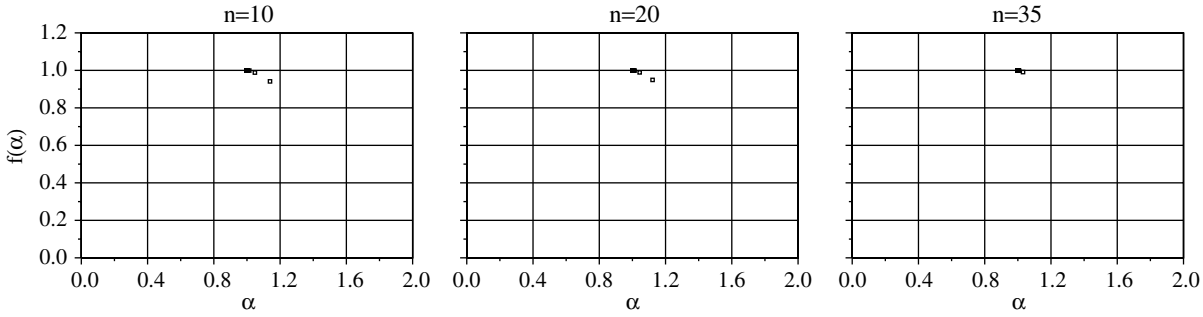

Figure 7. Mutifractal spectrum of parabola $g(x) = 2x - x^2$ on interval (0, 2) estimated using Chhabra–Jensen's algorithm by changing scale range from 1/2000 to n/2000 (number of data samples N = 2001)

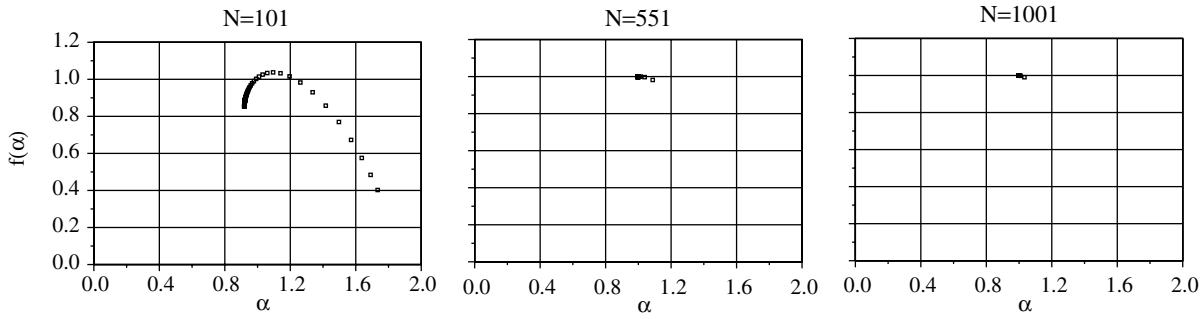

Figure 8. Multifractal spectrum of parabola $g(x) = 2x - x^2$ on interval (0, 2) estimated using Chhabra–Jensen's algorithm by changing the number of data samples N (scale range $1/(N-1)$ to $40/(N-1)$)

DEM contains only 275 data points with the minimum distance interval (the same as DEM resolution). In order to obtain enough data samples for applying the multifractal analysis, the extra data samples were obtained under the assumption of linear changes of width functions or area functions within the minimum distance interval. The following procedure was designed to obtain the 'real' singularity spectrum of the normalized width function or area function. Keeping on increasing the number of data samples and scale ranges by linear interpolation between two points up to the calculated spectrum tends to be stable. This stable spectrum is decided to be the 'real' spectrum. It should be recognized that validation of this procedure based on higher resolution DEMs is necessary.

Sensitivity of width function on the threshold areas

The multifractal spectra of width functions extracted from different threshold areas in all study catchments were calculated using the above proposed procedure. The variations of the spectra distinctly show the sensitivity of the width functions on threshold areas in the sense of their scaling characteristics. Figure 9 is an example from the Seki River. It can be seen that the spectrum changes drastically when the threshold area changes from 0·625 km^2 to 1 km^2, and tends to concentrate on the major part around point (1,1) when the threshold value is larger than 1·25 km^2. This trend is common for all study catchments. The results indicate that the river networks with larger threshold areas tend to lose some detailed scaling information. The river network generated by an appropriate threshold area should keep the catchment scaling structure and exclude the small unreal rivers. Therefore, the appropriate threshold area is specified to be the largest threshold value that keeps the catchment scaling structure. From the changes of the multifractal spectrums

shown in Figure 9, the appropriate threshold area is decided at 0·625 km^2 for the Seki River. Table I shows the appropriate threshold values of the study catchments. These values are related to the catchment area and slope irregularly.

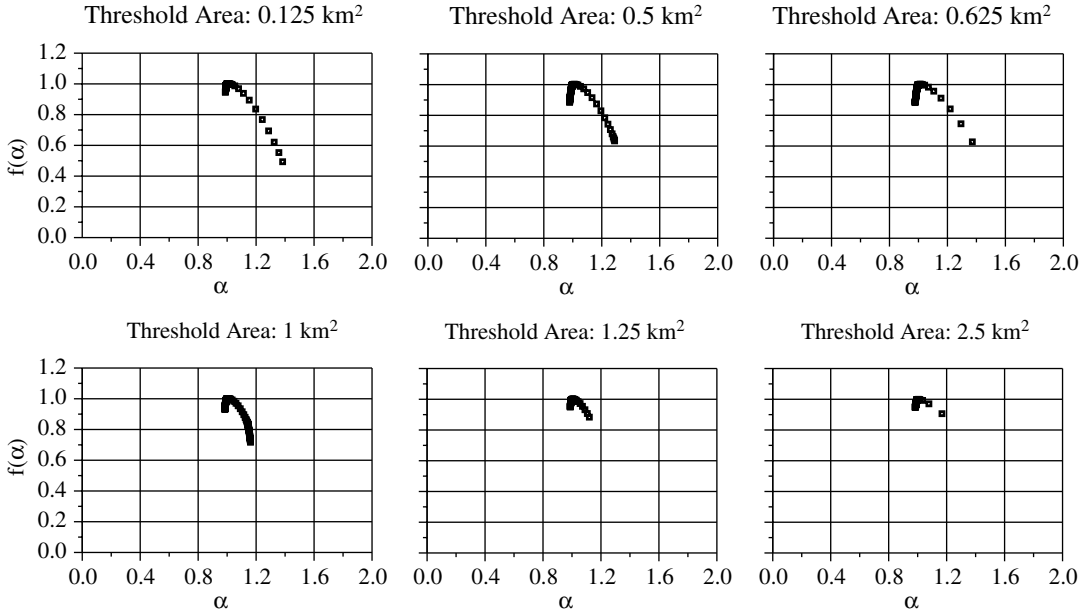

Figure 9. Multifractal spectra of width functions of the Seki River from different threshold areas

Table I. Threshold areas for river generation from DEMs

Catchment	Drainage area (km^2)	Average slope (%)	Threshold area (km^2)
Kyushu Region			
Chikugo River	2315	11·8	1·0
Oita River	601	13·9	0·25
Onga River	939	13·7	0·5
Oono River	1381	11·0	0·625
Yamakuni River	464	15·7	1·0
Shikoku Region			
Hiji River	984	20·3	0·25
Naka River	765	25·8	1·5
Niyodo River	1463	24·8	1·25
Yoshino River	3044	24·3	2·0
Kanto Region			
Agatsuma River	1239	18·3	0·25
Karasu River	1221	14·5	0·25
Watarase River	1209	11·9	0·625
Hokuriku Region			
Hime River	698	28·2	1·0
Kurobe River	637	38·1	1·0
Seki River	1133	16·0	0·625

Sensitivity of area function to the DEM resolutions

The singularity spectra of the area functions by DEMs of 250 m, 500 m and 1000 m resolutions are calculated for all the study catchments. Figure 10 gives an example from the Seki River. It was found that the spectrum becomes very narrow and focuses on the main part around point (1,1) when the DEM mesh size increases, and this variation is common to all study catchments. This suggests that increasing the DEM mesh size leads to losing the detailed scaling information in a catchment.

EFFECT OF DEM RESOLUTION ON HYDROLOGICAL SIMULATIONS BY THE GBHM

Effect on the topographical parameters used in the GBHM

In order to exclude the influences of water infrastructures (e.g. reservoir), the Naka River of Shikoku region and the Karasu River of Kanto region were selected to examine the effect of the DEM resolution on hydrological simulation by the GBHM. The topographical parameters used in GBHM include area function, width function, elevation and slope. The area function and width function are used to determine the sizes of hillslopes. Table II summarizes these parameters of the two study catchments extracted from different DEMs. It shows that the size of the hillslope element increases with an increase in the DEM mesh size. Because decreasing the hillslope width beyond the DEM resolution does not increase the accuracy of representation of catchment topography, the hillslope width (i.e. the flow interval length) is taken in the range between DEM resolution and two times the DEM resolution according to the length of the main river segment (Yang *et al*., 1998). The length of the hillslope increases with lower resolution DEMs due to the reduced river density. The elevation does not change much in different resolutions, but the slope becomes gentler in lower resolutions.

Effect on hydrological simulations

The hydrological simulations were carried out from 1992 to 1995 in both study catchments, and the simulated annual water balance is summarized in Table III. The total runoff tends to decrease and actual evaporation tends to increase with increasing the coarseness of the DEM grid size. This means that more water was stored in the subsurface zone in the case of coarser DEMs. From the daily hydrographs (see Figure 11), it can be found that increasing the DEM mesh size tends to increase the peak of high flow and decrease the low flow. This indicates that more saturated runoff but less subsurface runoff was generated using the coarser DEMs. Based on a DEM of lower resolution, the topography tends to be flattened, and the river network becomes sparser. The reduced slope and sparse river network cause decreasing runoff generation and increasing storage in the subsurface because of the assumptions taken in the GBHM that the impervious surface parallel to the hillslope and the number of hillslopes corresponds to the rivers.

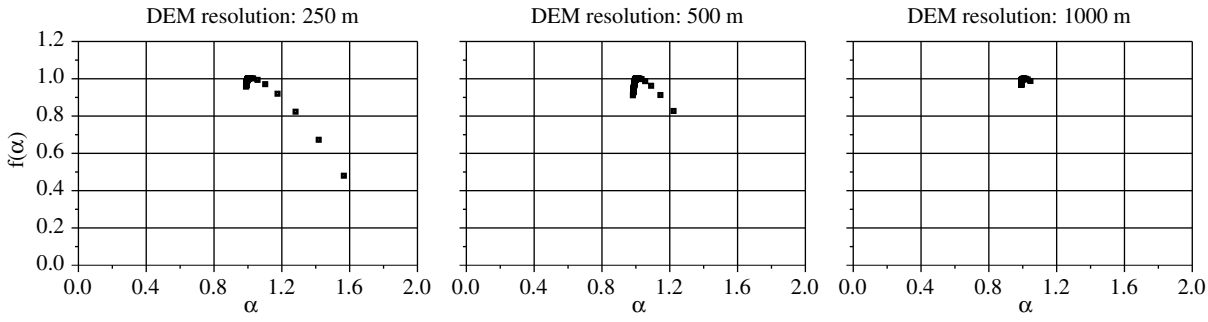

Figure 10. Multifractal spectra of area functions of the Seki River from DEMs of different resolutions

Table II. Topographical parameters in GBHM from different resolutions of DEMs

Catchment DEM resolution	Karasu River			Naka River		
	250 m	500 m	1000 m	250 m	500 m	1000 m
Discrete unit						
Number	3203	1623	370	677	379	166
Length × width (m)	469 × 416	606 × 653	1236 × 1330	980 × 454	1128 × 787	1423 × 1424
Area (km^2)	0·387	0·772	3·270	1·0	1·79	4·10
Elevation (m)						
Minimum	68·0	68·0	69·0	124·5	102·2	130·7
Maximum	1148·6	1205·9	1102·5	1373·9	1312·1	1179·5
Mean	455·9	452·8	436·8	638·2	638·4	640·8
Slope (°)						
Minimum	0·13	0·05	0·03	2·48	0·27	0·35
Maximum	14·97	10·99	7·10	20·50	16·35	11·34
Mean	6·97	5·07	3·57	13·83	9·56	5·67

Table III. Hydrological simulations by GBHM based on different resolutions of DEMs

Catchment DEM resolution	Karasu River			Naka River		
	250 m	500 m	1000 m	250 m	500 m	1000 m
1993						
Rainfall (mm)		1559·8			4637·9	
Runoff (mm)	838·0	814·2	793·2	3822·4	3416·9	3359·6
Evaporation (mm)	710·1	736·1	772·4	767·5	787·3	821·3
Runoff error (%)	3·47	1·67	−4·29	−3·1	−12·8	−14·0
1994						
Rainfall (mm)		1367·8			3066·5	
Runoff (mm)	682·7	659·4	638·5	2212·5	1834·4	1795·1
Evaporation (mm)	726·1	759·4	798·5	841·3	866·0	920·6
Runoff error (%)	16·7	14·0	6·7	−5·1	−19·0	−20·6
1995						
Rainfall (mm)		1441·5			2661·5	
Runoff (mm)	758·6	730·3	710·6	1825·1	1559·8	1530·2
Evaporation (mm)	708·1	736·2	773·3	815·6	839·7	881·1
Runoff error (%)	28·1	24·7	17·2	−9·3	−23·9	−25·2

In the same simulation, enlarging the hydrograph to look at the hourly variations of the hydrological response (Figure 12), it is found that the hydrological response becomes quicker when the DEM mesh size increases. This can be explained when the topography becomes smoother, subsurface flow decreases and more water is stored in the subsurface; therefore, less water is needed to saturate the subsurface soil, the saturated surface runoff responds faster. The pattern of total hydrological response is changed by the variation of the runoff generations from surface and subsurface affected by the topography. Comparing the daily and hourly hydrographs, it is found that the effect of the DEM resolution on the hydrological response is related to the temporal resolution. The influence to the hourly response is more significant than the daily response. This can be explained from the spatial resolution sensitivity of the area function. The pattern of hydrological response is related to the scaling property of a catchment that is expressed by the multifractal spectrum. The major property of the multifractal spectrum of the area function (in Figure 10) is kept in different spatial resolutions. This corresponds to a good matching of the general patterns of the simulated daily responses

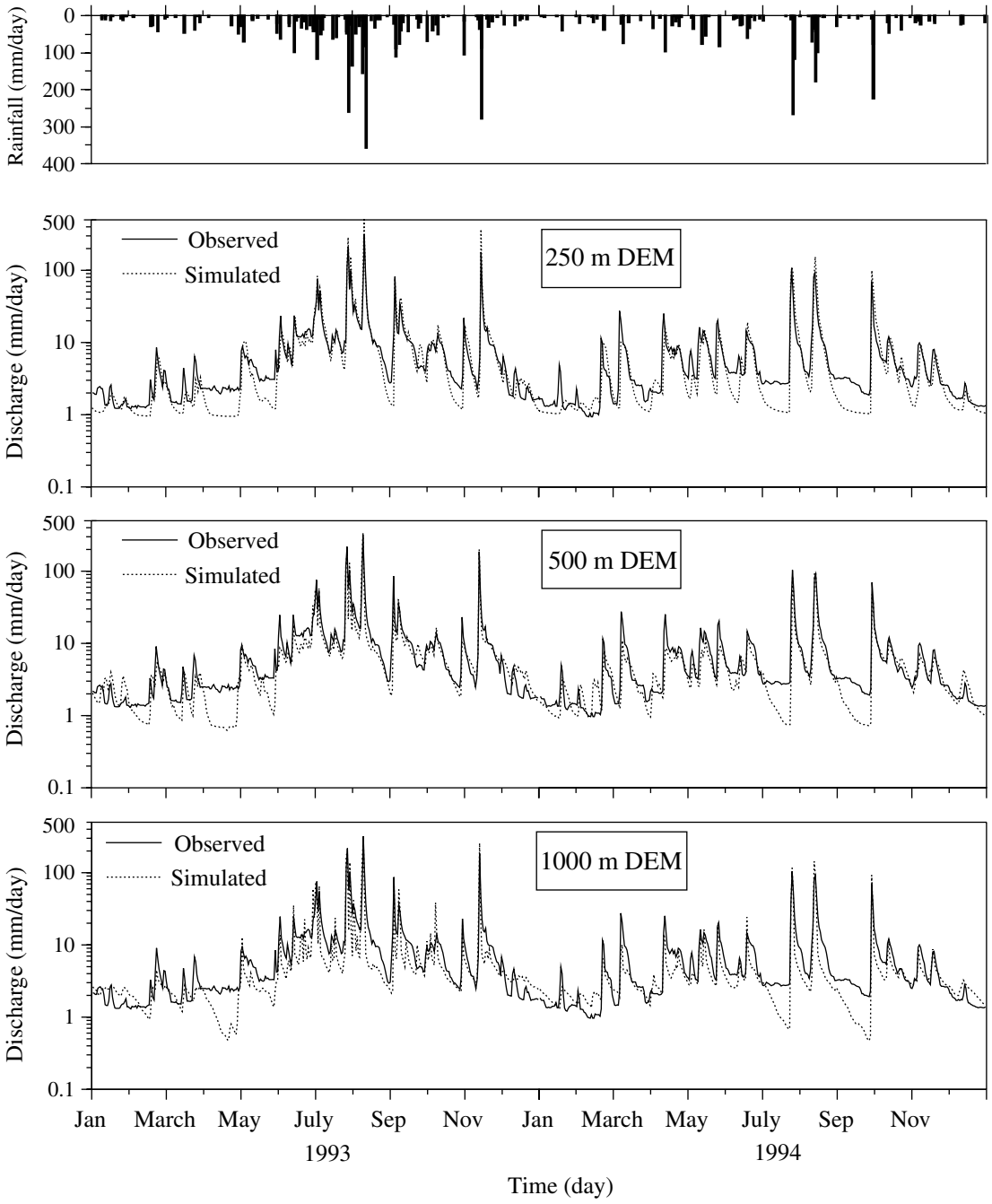

Figure 11. Daily hydrographs of the Naka River simulated by the GBHM using DEMs of different resolutions

using DEMs of different resolutions. The effect of detailed scaling information that is lost in the case of low spatial resolution (coarse mesh size) can only be seen from the hydrological responses of high temporal resolution. The hourly hydrological response had higher sensitivity to the DEM resolution compared with the daily response.

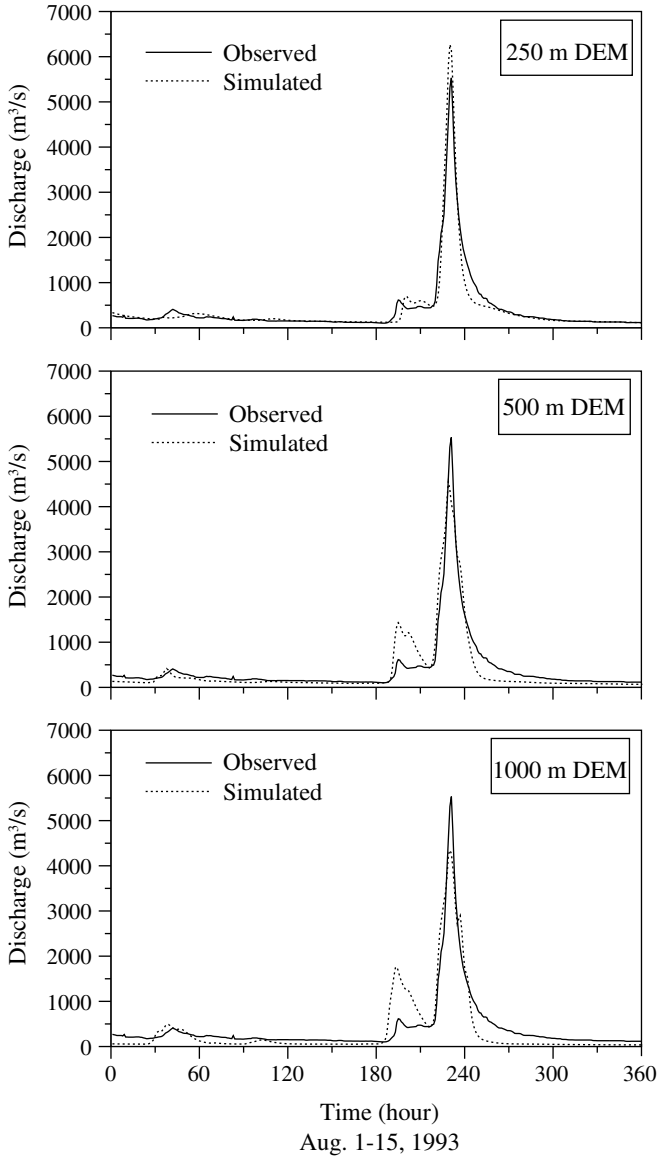

Figure 12. Hourly hydrographs of the Naka River simulated by the GBHM using DEMs of different resolutions

CONCLUSIONS

Horton's ratios and fractal dimension cannot show detailed scaling structure of a catchment, and they vary irregularly with respect to the threshold area and DEM resolution. The multifractal analysis offers a useful tool for investigating the sensitivity of the geomorphologic width function and area function that are used by the GBHM. On the river network generation, it was shown that the river networks generated with larger threshold areas tend to lose detailed scaling information. From the variations of the multifractal spectrum, the appropriate threshold area for river generation is decided to be the largest threshold value that keeps the catchment scaling structure. Increasing the DEM mesh sizes, the river networks extracted with the same threshold area become sparser and the topography tends to be smoother. The scaling structure of

the area function becomes simpler with lower spatial resolution. The procedure proposed for estimating the real multifractal spectrum of width function and area function needs to be validated using higher resolution DEMs.

The DEM resolution directly influences the runoff generation of the GBHM. The reduced slope and sparse river network cause decreasing runoff generation and increasing storage in the subsurface. It was found that the effect of the DEM resolution on the hydrological response is related to the temporal resolution. The influence of DEM resolution on the hourly response is more significant than the daily response. From the relation between the scaling structure expressed by the multifractal spectrum and the hydrological response of a catchment, it was found that the detailed scaling property had more effect on the hydrological response of higher temporal resolution. This implies that caution should be taken in the hydrological simulation using low resolution DEMs when high temporal resolution of the simulation is required.

REFERENCES

Barbera PL, Rosso R. 1989. On the fractal dimension of stream networks. *Water Resources Research* **25**: 735–741.

Beven K. 1989. Changing ideas in hydrology—the case of physically-based models. *Journal of Hydrology* **105**: 157–172.

Chhabra A, Jensen RV. 1989. Direct determination of the f(α) singularity spectrum. *Physical Review Letters* **62**: 1327–1330.

Dietrich W, Wilson C, Montgomery D, Mckean J. 1993. Analysis of erosion thresholds, channel networks and landscape morphology using a digital terrain model. *Journal of Geology* **101**: 259–278.

Feder J. 1998. *Fractals*. Plenum Press: New York.

Helmlinger KR, Kumar P, Foufoula-Georgiou E. 1993. On the use of digital elevation model data for Hortonian and fractal analyses of channel networks. *Water Resources Research* **29**: 2599–2613.

Herath S, Yang D, Musiake K. 1999. Description of catchment hydrological response using the catchment area function. *IAHS Publication* **254**: 61–70.

Ichoku C, Karnieli A, Verchovsky I. 1996. Application of fractal techniques to the comparative evaluation of two methods of extracting channel networks from digital elevation models. *Water Resources Research* **32**: 389–399.

Marani M, Rinaldo A, Rigon R, Rodriguez -Iterbe I. 1994. Geomorphological width functions and the random cascade. *Geophysical Research Letters* **21**: 2123–2126.

Maritan A, Rinaldo A, Rigon R, Giacometti A, Rodriguez-Iturbe I. 1996. Scaling laws for river networks. *Physical Review E* **53**: 1510–1515.

Mesa O, Mifflin E. 1986. On the relative role of hillslope and network geometry in hydrological response. In *Scaling Problems in Hydrology*, Gupta VK, Rodriguez-Iturbe I, Wood E (eds). Reidel: Dordrecht; 1–17.

Montgomery D, Foufoula-Georgiou E. 1993. Channel network source representation using digital elevation models. *Water Resources Research* **29**: 3925–3934.

Moore I, O'Loughlin E, Burch G. 1988. A contour based topographic model for hydrological and ecological applications. *Earth Surface Processes and Landform* **13**: 305–320.

Moore I, Grayson RB, Ladson AR. 1991. Digital terrain modelling: A review of hydrological, geomorphological and biological applications. *Hydrological Processes* **5**: 3–30.

Nikora VI, Sapozhnikov VB. 1993. River network fractal geometry and its computer simulation. *Water Resources Research* **29**: 3569–3575.

O'Callaghan JF, Mark DM. 1984. The extraction of drainage networks from digital elevation data. *Computer Vision, Graphics and Image Processing* **28**: 328–334.

Palacios-Velez O, Cuevas-Renaud B. 1986. Automated river-course, ridge and basin delineation from digital elevation data. *Journal of Hydrology* **86**: 299–314.

Rinaldo A, Rodriguez-Iturbe I, Rigon R, Ijjasz-Vasquez E, Bras RL. 1993. Self-organized fractal river networks. *Physical Review Letters* **70**: 822–825.

Robinson J, Sivapalan M, Snell J. 1995. On the relative roles of hillslope processes, channel routing, and network geomorphology in the hydrological response of natural catchments. *Water Resources Research* **31**: 3089–3101.

Strahler A. 1952. Hypsometric (area-altitude) analysis of erosional topography. *Bulletin of the Geological Society of America* **63**: 1117–1142.

Tarboton DG, Bras RL, Rodriguez-Iturbe I. 1991. On the extraction of channel networks from digital elevation data. *Hydrological Processes* **5**: 81–100.

Veneziano D, Moglen GE, Bras RL. 1995. Multifractal analysis: pitfalls of standard procedures and alternatives. *Physical Review E* **52**: 1387–1398.

Walker JP, Willgoose GR. 1999. On the effect of digital elevation model accuracy on hydrology and geomorphology. *Water Resources Research* **35**: 2259–2268.

Wolock D, Price C. 1994. Effect of digital elevation model map scale and data resolution on a topography-based watershed model. *Water Resources Research* **30**: 3041–3052.

Yang D, Herath S, Musiake K. 1997. Analysis of geomorphologic properties extracted from DEMs for hydrological modeling. *Annual Journal of Hydraulic Engineering, JSCE* **41**: 105–110.

Yang D, Herath S, Musiake K. 1998. Development of a geomorphology-based hydrological model for large catchments. *Annual Journal of Hydraulic Engineering, JSCE* **42**: 169–174.

Yang D, Herath S, Musiake K. 2000. Comparison of different distributed hydrological models for characterization of catchment spatial variability. *Hydrological Processes* **14**: 403–416.

Yen B, Lee K. 1997. Unit hydrograph derivation for ungauged watersheds by stream-order laws. *Journal of Hydrologic Engineering, ASCE* **2**: 1–9.

Zhang W, Montgomery D. 1994. Digital elevation model grid size, landscape representation, and hydrologic simulation. *Water Resources Research* **30**: 1019–1028.

